Title
ROM mapping of ligamentous constraints on avian hip mobility: implications for extinct ornithodirans

Journal
Proceedings of the Royal Society B, 285(1879)

ISSN
0962-8452

Authors
Manafzadeh, Armita R
Padian, Kevin

Publication Date
2018-05-30

DOI
10.1098/rspb.2018.0727

Peer reviewed

PROCEEDINGS B

rspb.royalsocietypublishing.org

Research

Cite this article: Manafzadeh AR, Padian K. 2018 ROM mapping of ligamentous constraints on avian hip mobility: implications for extinct ornithodirans. *Proc. R. Soc. B* **285**: 20180727. http://dx.doi.org/10.1098/rspb.2018.0727

Received: 1 April 2018
Accepted: 27 April 2018

Subject Category:
Morphology and biomechanics

Subject Areas:
biomechanics, palaeontology

Keywords:
range of motion, joint mobility, hip ligaments, avian functional morphology, Ornithodira, Pterosauria

Author for correspondence:
Armita R. Manafzadeh
e-mail: armita_manafzadeh@brown.edu

Electronic supplementary material is available online at https://dx.doi.org/10.6084/m9.figshare.c.4092521.

THE ROYAL SOCIETY PUBLISHING

ROM mapping of ligamentous constraints on avian hip mobility: implications for extinct ornithodirans

Armita R. Manafzadeh[1] and Kevin Padian[2]

[1]Department of Ecology and Evolutionary Biology, Brown University, Providence, RI, USA
[2]Department of Integrative Biology and Museum of Paleontology, University of California, Berkeley, CA, USA

ARM, 0000-0001-5388-7942; KP, 0000-0002-1174-8431

Studies of soft tissue effects on joint mobility in extant animals can help to constrain hypotheses about joint mobility in extinct animals. However, joint mobility must be considered in three dimensions simultaneously, and applications of mobility data to extinct taxa require both a phylogenetically informed reconstruction of articular morphology and justifications for why specific structures' effects on mobility are inferred to be similar. We manipulated cadaveric hip joints of common quail and recorded biplanar fluoroscopic videos to measure a 'ligamentous' range of motion (ROM), which was then compared to an 'osteological' ROM on a ROM map. Nearly 95% of the joint poses predicted to be possible at the hip based on osteological manipulation were rendered impossible by ligamentous constraints. Because the hip joint capsule reliably includes a ventral ligamentous thickening in extant diapsids, the hip abduction of extinct ornithodirans with an offset femoral head and thin articular cartilage was probably similarly constrained by ligaments as that of birds. Consequently, in the absence of extraordinary evidence to the contrary, our analysis casts doubt on the 'batlike' hip pose traditionally inferred for pterosaurs and basal maniraptorans, and underscores that reconstructions of joint mobility based on manipulations of bones alone can be misleading.

1. Introduction

Reconstructions of joint mobility for extinct taxa have traditionally relied solely on information from the physical or digital manipulation of fossil bones (e.g. [1–5]). By studying interactions between fossilized pairs of 'articular' surfaces (see [6–8]), palaeontologists have estimated ranges of motion (ROM) limited by only two criteria: bone-on-bone stops and disarticulation.

However, the appendicular joints of vertebrates are well-integrated systems that—in addition to bone—also comprise soft tissues such as cartilage, ligaments, muscles, tendons, connective tissues, and the nerves and vessels that supply them [9]. This presents a problem for palaeontologists because articular soft tissues, which are typically not preserved in the fossil record, substantially affect joint mobility. Functional morphologists have recently begun to quantify these effects (e.g. [10], electronic supplementary material; [11–20]), often with the intent of applying the data to palaeobiological reconstructions. Although such analyses have considerable potential to help to constrain hypotheses about joint mobility in extinct animals, we suggest that they would benefit from certain philosophical and methodological improvements.

Philosophically, justifications beyond the use of a simple extant phylogenetic bracket (EPB) [21] are necessary to apply mobility data from a joint in an extant animal to the reconstruction of a particular joint in an extinct animal. The morphology, and thus the effect on mobility, of articular structures varies both among joints and among animals (and even in the same individual developmentally). For example, substantial differences are evident in the knees of birds and crocodiles, which form the EPB for all extinct archosaurs. In birds,

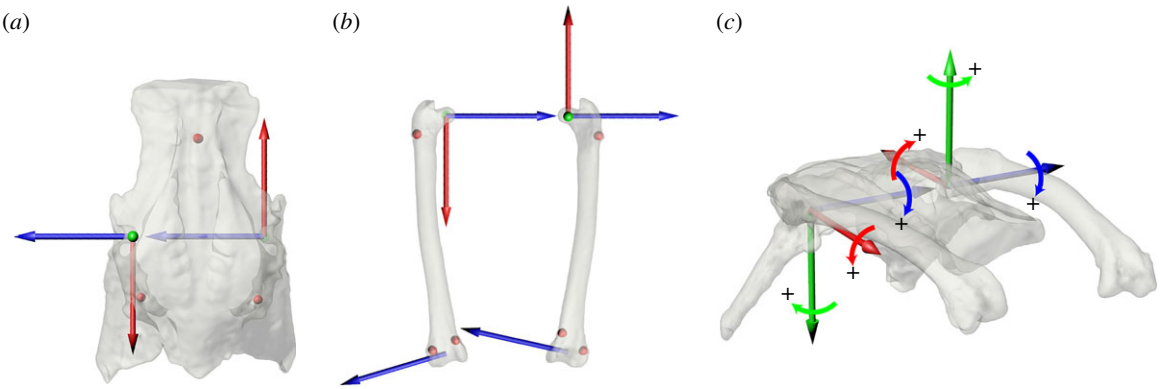

Figure 1. The anatomical coordinate systems for the (*a*) pelvis (dorsal view) and (*b*) femora (dorsal view), and (*c*) the resulting hip joint coordinate systems shown in the reference pose (all rotations equal zero; anterolateral view). Red spheres in (*a*,*b*) represent radiopaque marker implantation sites. Plus signs in (*c*) indicate conventions for positive rotations in each degree of freedom, where rotation about blue is FE, green is ABAD, and red is LAR.

the distal condyles of the femur are more strongly defined, there are more intra-articular structures, and the epiphyses of the long bones retain far less cartilage than in crocodiles [7,8,22,23]. Knowledge of soft tissue effects on mobility in one joint does not necessarily allow strong prediction of those in others, even in closely related taxa (e.g. [14]).

In practice, methods used to measure and report ROM must be pose-based in order to capture the 3D complexity of joint mobility adequately. Joint motions have historically been decomposed into discrete degrees of freedom (DoF), such as flexion–extension (FE), abduction–adduction (ABAD) and long-axis rotation (LAR), and ranges of excursion in each of these DoF have been considered independently. However, recent functional studies of joints have demonstrated that the range of excursions possible in one DoF strongly depends on simultaneous excursions in the others [24]. In disregarding these interactions, studies that measure and report separate ranges of excursion for each DoF incorrectly suggest the viability of combinations of rotations (i.e. joint poses) that are never achieved. Separate bar graphs for each DoF are an inadequate visualization, and percentage differences for each DoF are an inadequate calculation, for reporting biologically meaningful ROM data (see [24] for a more extensive discussion).

Here we develop an approach that we call 'ROM mapping' to visualize and compare joint mobilities. We analyse as an example the hip joint mobility of the common quail, as (i) predicted from dry bones alone, using new automated methods of generating bone–bone configurations and checking for mesh model interpenetration, and (ii) experimentally measured from cadaveric quail with intact hip joint capsules, using biplanar fluoroscopy. We then infer quail hip ligament functions using a new method of dynamic ligament simulation, and discuss the implications of our results for reconstructing hip joint mobility in extinct ornithodirans (bird-line archosaurs).

2. Material and methods

(a) Dissection

The common quail was selected for study because it is a terrestrially proficient basal Neornithine [25]. Three fresh frozen adult common quail (*Coturnix coturnix*; QROM01–QROM03), obtained from RodentPro.com, LLC (Evansville, IN, USA), were dissected to isolate the vertebral column, pelvis and femora. All muscles were removed under a Wild Heerbrugg (Wild of Canada Ltd., Ottawa, Canada) or Nikon SMZ800 (Nikon Corporation, Tokyo, Japan) stereomicroscope at 10–60× magnification to ensure integrity of the hip joint capsule. A fourth individual, used only for anatomical study, was dissected further to allow examination of structures within the hip joint capsule.

(b) 'Ligamentous' hip ROM measurement

To measure a 'ligamentous' ROM (i.e. the range of motion of the hip with the joint capsule intact), we used biplanar fluoroscopy. Radiopaque markers (0.8 mm diameter zirconium oxide ball bearings; Ortech, Inc., Sacramento, CA, USA) were press-fitted into hand-drilled holes in the ilia and femora (three per bone; see figure 1*a*,*b*) of individuals QROM01–QROM03, and affixed with cyanoacrylate adhesive. Each specimen was mounted in the centre of the X-ray volume created by two X-ray image systems (Imaging Systems and Service, Painesville, OH, USA) comprising two Varian model G-1086 X-ray tubes (75–85 kV, 200 mA, magnification level 3, 2 ms pulse width) and two Dunlee model TH9447QXH590 image intensifiers (96–124 cm SID) in the W. M. Keck Foundation XROMM Facility at Brown University. A 3.175 mm × 0.914 m wooden dowel was fastened to each femur using three 5 mm × 10 cm cable ties to allow the researcher to manipulate the hip joint from a safe distance outside the X-ray volume. A total of 38 biplanar fluoroscopic videos of the hip joints taken through extremes of rotation was recorded (10 fps, 1/1000 s shutter speed, 1760 × 1760 resolution) using Phantom v.10 high-speed cameras (Vision Research, Wayne, NJ, USA). Extremes of rotation were determined based on researcher sensation of a hard stop caused by ligamentous constraints, as described by Kambic *et al*. [24]. Still X-ray images of a standard grid and an object of known geometry were also captured to allow undistortion and 3D calibration of the cameras [26,27].

Following video data collection, specimens were disarticulated and computed-tomography scans (90 kV, 0.1 mA, 0.173 mm slice thickness, 480 × 480 resolution; FIDEX CT, Animage, Pleasanton, CA, USA) were taken of the pelves and femora. All calibration images, X-ray videos, and CT files were uploaded to the X-ray Motion Analysis Research Portal, a web environment for the storage, management, and sharing of XROMM data (xmaportal.org), and are publicly available. Mesh models of skeletal elements and radiopaque markers were reconstructed using Amira v. 6.0.1 (Mercury Systems, MA, USA) and cleaned using Geomagic Studio 2013 (3D Systems, Morrisville, NC, USA), where geometric primitives were fit to the acetabulum, femoral head, and distal femoral condyles. Models and primitives were imported into Maya 2016 (Autodesk, San Rafael, CA, USA), and coordinate systems and reference poses were generated following Kambic *et al*. [28] (figure 1).

X-ray videos were calibrated and digitized using XMALab v. 1.5.0 [27]; the precision of tracking was 0.0386 mm (mean s.d. of intermarker distance for 228 co-osseous marker pairs over 38

trials; see [26]). Rigid body transformations were computed and used to animate bone models in Maya, where six DoF kinematics were calculated from joint coordinate systems [29] using the 'Output Relative Motion' script in the XROMM_MayaTools package (available at xromm.org). This process yielded 20 627 measured hip poses: 4195 from individual QROM01 (2123 left and 2072 right); 6206 from QROM02 (2803 left and 3403 right); and 10 226 from QROM03 (4826 left and 5400 right).

(c) 'Osteological' hip ROM measurement

To simulate palaeobiological reconstruction of hip mobility and measure an 'osteological' ROM (i.e. the range of motion of the hip predicted from dry bones only), we created an automated system for generating millions of bone–bone configurations and checking them for mesh model interpenetration. This method eliminates the risk of inter-observer differences in ROM estimation (see [12]) by standardizing the search process. A forward kinematic model was created in Maya 2016 (Autodesk, San Rafael, CA, USA) by constraining the femur mesh model of individual QROM01 to a character animation joint created based on the same joint coordinate system used for 'ligamentous' ROM measurement. This joint was centred inside the individual's right acetabulum and then translated up to 2 mm laterally, 1 mm dorsally and 1 mm ventrally in increments of 0.5 mm, resulting in 25 combinations of hip joint translations. These values were selected because lateral translation beyond 2 mm would have situated the femoral head entirely outside the acetabulum, dorsoventral translation beyond 1 mm always resulted in interpenetration of the femur and pelvis, and anteroposterior translation of 0.5 mm often resulted in interpenetration and never yielded any viable poses beyond those captured using the 25 translation combinations detailed above.

At each hip joint translation, the femur was animated to sample all potential combinations of hip joint rotations (−180° to 180° FE, −90° to 90° ABAD, −180° to 180° LAR) at a resolution of five degrees (186 624 poses). Certain regions of joint pose space were further sampled at one-degree resolution to ensure complete coverage, resulting in an additional 54 000 poses tested (see Results). Thus, 240 624 poses were generated at each of 25 translations, yielding a total of 6 015 600 femur-pelvis configurations tested. Polygonal Boolean operations were applied to pelvis and femur mesh models at each configuration, and the surface areas of the resulting intersection meshes were queried to search for poses that did not result in bone-on-bone interpenetration. Using this method, 42 131 viable 'osteological' poses were found. A simple random sample of 1000 poses was manually checked to ensure viability; no sampled pose was inaccurate. The MEL code used in this study, and generalized instructions for sampling joint poses and creating an automated system to check for mesh model interpenetration in Maya, are provided as electronic supplementary material, methods S1 and S2.

(d) ROM mapping

We developed an approach that we call ROM mapping, building on the methods created by Kambic *et al*. [24], to allow visualizations and measurements of joint mobility that capture its 3D complexity. Making a 'ROM map' involves (i) plotting 3D points representing each joint pose in a space representing all possible poses, and then (ii) wrapping the resulting point cloud as tightly as possible to create a polygonal ROM envelope representing a joint's mobility (see electronic supplementary material, movie S1 for a visual guide to understanding ROM mapping). If several mobilities are measured using the same joint coordinate system—for example, our 'ligamentous' and 'osteological' mobilities—they can be placed on the same ROM map, and the relative extent and overlap of their ROM envelopes can be visualized and computed. This process can be thought of as analogous to charting the areas of various countries and continents on a political map. A political map allows a cartographer to calculate how much of Africa is taken up by Botswana, compare the sizes of Denmark and China, or measure the distance separating Mexico from Argentina. In the same way, a ROM map is a visualization that makes it possible to compare several nested mobilities from the same animal, or even mobilities measured from different ones.

In the present study, we created our ROM map by importing the FE, ABAD and LAR angle values measured from the joint coordinate system for each 'ligamentous' and 'osteological' hip pose into MatLab R_2017a (Mathworks, Natick, MA, USA) and plotting them as points in an Euler angle-angle-angle space with a total volume of 23 328 000 degrees^3. An alpha shape—a three-dimensional polygonal envelope that captures the external shape of a point cloud—was computed for the sets of 'ligamentous' and 'osteological' poses. Because there is no reason to presume convexity of joint pose point clouds (*pace* [24]), alpha radii were set to produce the tightest fitting alpha shapes that enclosed all points without allowing internal holes. The volumes of the resulting 'ligamentous' and 'osteological' ROM envelopes were computed using native MatLab functions and compared. The MatLab code used in this study, and generalized instructions for creating a ROM map in MatLab, are provided as electronic supplementary material, method S3.

(e) Dynamic ligament fibre simulation

Because *in vivo* measurement of ligament length remains challenging, we developed a new method of dynamic ligament fibre simulation to explore hip ligament function in the common quail. Pubofemoral and ventral and caudal ischiofemoral ligament fibres were modelled as polygonal meshes and constrained to their attachment sites (as determined in our dissections; see electronic supplementary material, figure S3) on the femur and pelvis mesh models of individual QROM03 in Maya 2016 (Autodesk, San Rafael, CA, USA). Bone penetration was avoided (i.e. ligament fibres were forced to wrap around the pelvis and femur) using an nCloth dynamic simulation. Fibre lengths were computed at all hip poses measured from QROM03, and also in a roughly 'batlike' hip pose, defined here as (FE°, ABAD°, LAR°) = (90, 70, 0). Because true ligament resting length could not be measured, ligament fibre recruitment—length at a given pose as a percentage of maximum length reached—was calculated for all poses (see [30]). Correlations between recruitment and hip rotational degrees of freedom for each modelled fibre were then calculated to determine which motions the fibres were most involved in limiting. The nCloth properties and MEL code used in this study, and generalized instructions for creating a dynamic ligament fibre simulation in Maya, are provided as electronic supplementary material, method S4.

3. Results

(a) Anatomical description of the hip joint capsule

The avian hip joint capsule has traditionally been described as comprising three ligamentous thickenings: the iliofemoral, ischiofemoral and pubofemoral ligaments [31]. In this study, the pubofemoral ligament was found to be the only capsular ligament whose caudal and rostral borders are consistently demarcated. In the quail, this ligament is a distinct, fibrous, band-like thickening of the hip joint capsule originating at the pubic peduncle of the ilium and inserting on the rostrolateral femoral metaphysis. The ischiofemoral ligament is a less distinct thickening of the capsule originating at the ventrocaudal acetabular rim and inserting on the medial and caudal femoral metaphysis. Baumel & Raikow [31] suggested that the iliofemoral ligament originates on the dorsal

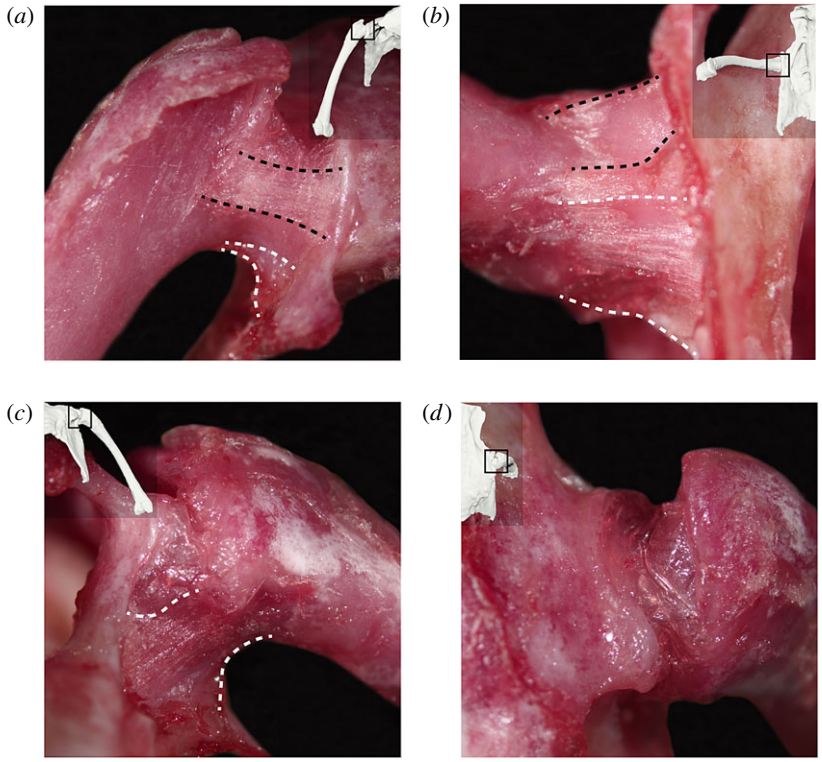

Figure 2. Images of the hip joint capsule and its ligamentous thickenings in the right hip of a common quail: (*a*) anterior, (*b*) ventral, (*c*) posterior and (*d*) dorsal views. Thumbnails in each view display the approximate hip pose at which each image was taken. Black dashed lines indicate the borders of the pubofemoral ligament; white dashed lines indicate the approximate borders of the ischiofemoral ligament. (Online version in colour.)

acetabular rim and inserts onto the trochanteric extent of the femoral articular surface. However, the current study, our previous dissection of *Gallus* [20], and dissections of other galliforms and *Buteo*, *Cathartes* and *Corvus* by Tsai & Holliday [32] did not find the iliofemoral ligament to be a reliably present thickening of the capsule. Although the descriptive literature spans over half a century, images of an intact avian hip joint capsule and its ligaments do not exist, so we provide them here (figure 2).

Our observations of the quail are largely consistent with previous studies of other adult birds [20,31–35]. The joint capsule was found to be relatively thin and transparent dorsally, but reinforced by ligamentous thickenings both rostrally and ventrally. Within the capsule, a single ligamentum capitis femoris originates from the inner acetabular rim and inserts on the fovea capitis of the femoral head. The articular cartilage of the femur and acetabulum is very thin.

(b) 'Ligamentous' hip ROM description

The possible locations of the quail distal femur with the hip joint capsule intact, based on pooled measurements from all six hips to ensure complete sampling, are represented as small spheres in figure 3. Inter-individual differences among the hips studied were minimal and are displayed in electronic supplementary material, figure S1 (see [24] for a discussion of potential sources of variation; differences in the present study are mostly attributed to the differing number of poses sampled per hip.). The position of each sphere in figure 3 captures the FE and ABAD of the hip, and hip LAR is represented by sphere colour, where a darker colour indicates a more externally rotated hip pose (high LAR) and a lighter colour indicates a more internally rotated hip pose (low LAR).

(c) ROM map comparison of 'ligamentous' and 'osteological' hip mobilities

A ROM map including 'ligamentous' and 'osteological' hip mobilities of the common quail is displayed in figure 4. The volume of the outer 'osteological' ROM envelope (grey) is 5 408 052.67 degrees^3, whereas the volume of the enclosed 'ligamentous' ROM envelope (teal) is only 285 563.63 degrees^3. In other words, 94.72% of the hip joint poses that are contained within the 'osteological' envelope fall outside the 'ligamentous' envelope. Although these poses appear possible from the manipulation of bones alone, they are rendered impossible when the hip joint capsule is intact. We recognize that many of the poses in the 'osteological' envelope would never be considered by any morphologist attempting to reconstruct hip mobility in an extinct animal (e.g. Figure 4*a*). However, because in palaeobiological reconstructions there are no consistent methodological constraints on hypothesized mobility except bone-on-bone stops and disarticulation, this first approximation is not as much of a straw man as it may seem. Even if all poses with FE less than 0° (i.e. with the distal femur raised above the vertebral column) are eliminated, 89.30% of the remaining 'osteological' poses still lie outside the 'ligamentous' ROM envelope.

At certain locations in the ROM map, the 'osteological' ROM envelope does not extend beyond the 'ligamentous' envelope. In our simulation, this region was sampled at one-degree resolution to ensure more complete coverage of the 'osteological' envelope. The poses represented by these locations involve femur-on-antitrochanter interactions. However, for the most part, the striking disparity between the 'ligamentous' and 'osteological' envelopes indicates that ligaments play a large role in constraining avian hip mobility,

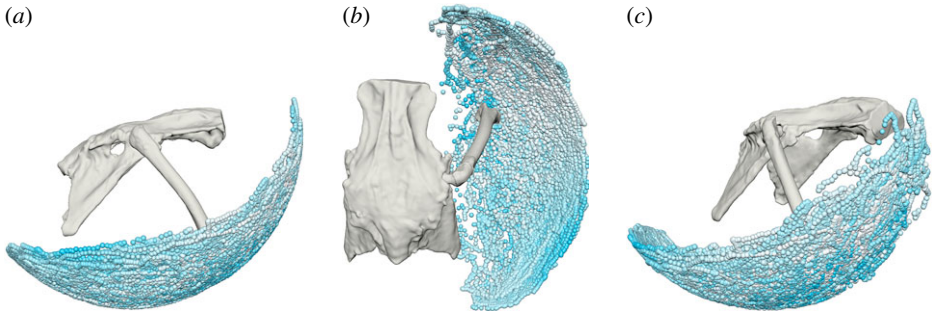

Figure 3. Possible locations of the distal femur with the hip joint capsule intact, represented by spheres relative to a right hip joint. Data pooled from all six hip joints studied and coloured by hip long-axis rotation at each point, where darker is more externally rotated and lighter is more internally rotated. (*a*) Lateral, (*b*) dorsal and (*c*) anterolateral views. (Online version in colour.)

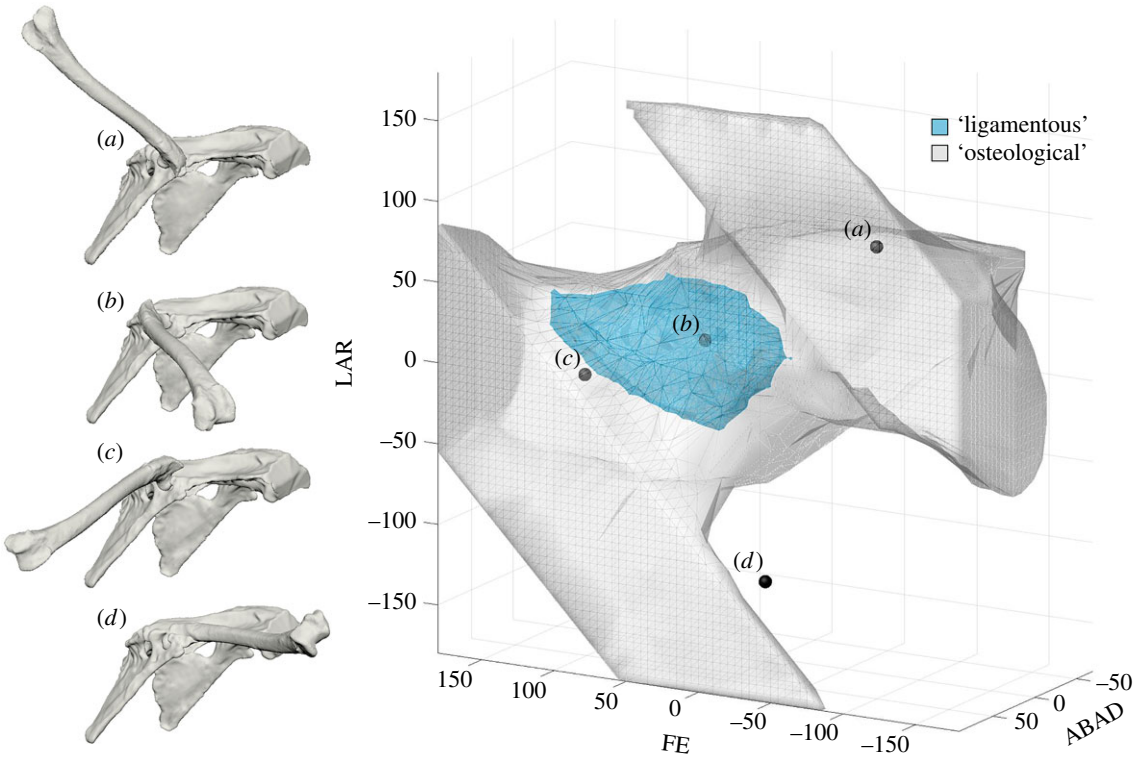

Figure 4. Four right hip poses of the common quail corresponding to the following (FE°, ABAD°, LAR°) triplets: (*a*) viable but biologically unreasonable (−100, 50, 100); (*b*) viable and possible with joint capsule intact (30, 30, 20); (*c*) bat-like (90, 70, 0); and (*d*) inviable (0, 10, −130). The 3D points representing these poses are plotted on a ROM map containing 'osteological' (grey) and 'ligamentous' (teal) quail hip ROM envelopes. A visual guide to interpreting this figure is provided as electronic supplementary material, movie S1. The map is viewed from an (azimuth°, elevation°) viewpoint of (210, 15); electronic supplementary material, figure S2 and movie S2 include other views. (Online version in colour.)

confirming the preliminary observations of Stolpe [33] and predictions of Rankin *et al*. [36].

(d) Ligament fibre recruitment

Ligaments restrict mobility in all three dimensions simultaneously, and their recruitment depends on excursions in all three degrees of freedom. Bearing this in mind, correlations between recruitment of simulated fibres and specific degrees of freedom can still indicate which excursions are most strongly limited by a given ligament. The pubofemoral ligament primarily limits external rotation at the hip joint ($r = 0.70$; see electronic supplementary material, figure S4*c*). The caudal ($r = 0.56$; see electronic supplementary material, figure S4*e*) and ventral ($r = 0.52$; see electronic supplementary material, figure S4*h*) fibres of the ischiofemoral ligament primarily limit abduction. These results support intuitive hypotheses of inferred function based on fibre orientation. To place the quail hip in a batlike pose of (FE°, ABAD°, LAR°) = (90, 70, 0), which lies outside the 'ligamentous' ROM envelope, the ventral fibres of the ischiofemoral ligament would need to stretch nearly 63% beyond their maximum experimental length (i.e. reach 162.8% recruitment).

4. Discussion

(a) Ligamentous constraints on avian hip mobility

Our analyses show that ligaments significantly constrain avian hip mobility. Because adult avian articular cartilage is very thin, the dramatic differences between the 'ligamentous'

and 'osteological' ROM envelopes found in our ROM map comparison can be attributed to the ligaments themselves. Consequently, when palaeobiological reconstructions of animals with similarly thin articular cartilage neglect ligamentous constraints, they probably overestimate joint mobility by a significant margin (for a consideration of the effects of thick articular cartilage, see [12]). The severity of this overestimation is obscured when comparisons of joint mobility are reduced to measurement of excursions in individual degrees of freedom. Dry bones alone gave an estimate of LAR of −180° to 180°, ABAD of −70° to 90° and FE of −180° to 180°, whereas with the hip joint capsule intact, only a LAR of −33.81° to 52.79°, an ABAD of −11.76° to 60.50° and a FE of −15.77° to 141.89° were possible. This translates to losses of only 75.95%, 54.84% and 56.21% respectively in each DoF, as compared to the 94.72% loss of joint poses determined through our ROM map comparison. The disparity between these metrics reinforces the importance of a pose-based analysis that considers joint mobility in three dimensions simultaneously, and underscores the utility of ROM mapping.

(b) Applying mobility data to extinct animals

Functional reconstructions of extinct animals rely on the premise that their joints could assume certain poses. However, even after a decade of great progress in investigating the effects of soft tissues on joint mobility (e.g. [10,12–19]), palaeobiologists still lack an explicit philosophical methodology for applying these data to extinct animals.

Of course, some extinct animals have limbs so different from those of their closest living relatives (e.g. the paddles of plesiosaurs, the wings of pterosaurs) that recourse to analogy is inevitable when discussing their joints. That said, there is general agreement that, whenever possible, homology is a better guide than analogy for reconstruction. This principle has led some workers (e.g. [21,37]) to lay out formal methods for reconstructing soft anatomical traits, and phylogenetically rigorous applications of these methods have allowed reconstructions of unpreserved articular morphology (e.g. [8,32,38]). Regrettably, the full complexity of joint anatomy has not typically played a role in reconstructions of joint mobility, which have instead relied on a dilution of Witmer's [21] EPB approach and used simple triangulation between mobility data from a bracket of two extant relatives, or even wholesale application of mobility data from a single extant relative.

Because the morphology of articular structures varies substantially, even among closely related taxa, the effects on mobility of those articular structures is also likely to vary substantially. Thus, it is insufficient to examine, for example, the effects of 'layers' (e.g. all integument, all muscles and tendons, all joint capsules and ligaments) of soft tissues on joint mobility in a bird and/or crocodile and use those data to make statements about joint mobility in any given extinct archosaur. Instead, further explanations are necessary for why the effects on mobility of the specific articular structures studied are inferred to be similar between an extant animal and its particular extinct relative. We suggest that in general, stronger reconstructions of mobility will involve an integration of data from (i) a detailed, structure-by-structure phylogenetic analysis of joint soft tissues, founded on the osteological correlates of articular morphology, and (ii) a functional analysis of how these specific soft tissue structures affect joint mobility. An application of this approach, using the data acquired in this study, follows below.

(c) Implications of quail ROM mapping for reconstructing ornithodiran hip mobility

Several extinct ornithodirans have been reconstructed with a 'batlike' hip pose in which the hip joints are severely abducted to include the hindlimbs in an aerofoil. This pose is nearly ubiquitous in reconstructions of pterosaurs (e.g. [39–42]; but see [3] for an opposing view), for whom its origin can be traced to Von Soemmering's [43] erroneous reconstruction of a juvenile *Pterodactylus* as a reptilian bat (figure 5*a*; see [46]). A similar hip pose has also been proposed for *Microraptor* and other basal maniraptorans (e.g. [45,47,48]), and is often associated with hypotheses about 'four-winged' gliding.

In our ROM map comparison of 'osteological' and 'ligamentous' mobilities in the common quail, a batlike pose of roughly (FE°, ABAD°, LAR°) = (90, 70, 0) fell within our 'osteological' ROM envelope, but outside our 'ligamentous' envelope (see figure 4*c*; electronic supplementary material, movie S1). In other words, although bony morphology alone permitted a batlike hip pose in the quail, the ligaments of the hip joint limited abduction enough to prevent it. Recall that our ligament fibre simulations demonstrated that to achieve this pose, the ventral fibres of the ischiofemoral ligament would have had to stretch nearly 63% beyond their maximum experimental length. The nearest neighbour of the batlike pose that fell within our 'ligamentous' envelope was (86.84, 57.00, 5.82), which lies a Euclidean (but see [49]) distance of 14.59° away. Although the hip joint was, in some poses, able to be further abducted (to a maximum of ABAD° = 60.50), the simultaneous FE and LAR excursions at these poses made them more different from (90, 70, 0), and the level of abduction reached was still insufficient to be classically batlike.

The hip joints of birds, pterosaurs and basal maniraptorans are osteologically similar in several respects. Notably, these taxa share medially oriented femoral heads (in contrast to bats; figure 5*b*; see [3,50,51] for an explanation of how bats adopt their hip pose) with thin articular cartilage. The femoral head was deflected medially over the course of theropod evolution [52,53]; pterosaurs independently underwent a comparable deflection [54]. In these extinct ornithodirans, just as in the common quail, the pelvis and femur can be manipulated to place the hip in a batlike pose. But the disparity between 'osteological' and 'ligamentous' hip mobilities in the common quail raises the question of whether manipulations of fossil bones have been misleading, and whether ligamentous constraints would, in life, also prevent this seemingly possible pose in pterosaurs and basal maniraptorans. To address this question, the effects on mobility of the hip capsular ligaments in these taxa must be considered.

Ligaments are passive structures that constrain joint mobility based on a combination of (i) their placement, which determines in what directions they restrict motion, and (ii) their resting length and material properties, which determine to what degree they do so [55]. Because hip capsular ligaments do not reliably leave direct scars on fossils, the placement of ligamentous thickenings in the hip joint capsules of extinct animals must be inferred based on data from dissections of their extant relatives. A detailed phylogenetic analysis of osteological correlates of hip soft tissues in dinosauromorphs by Tsai *et al*. [38] (see also [56]) concluded that extinct

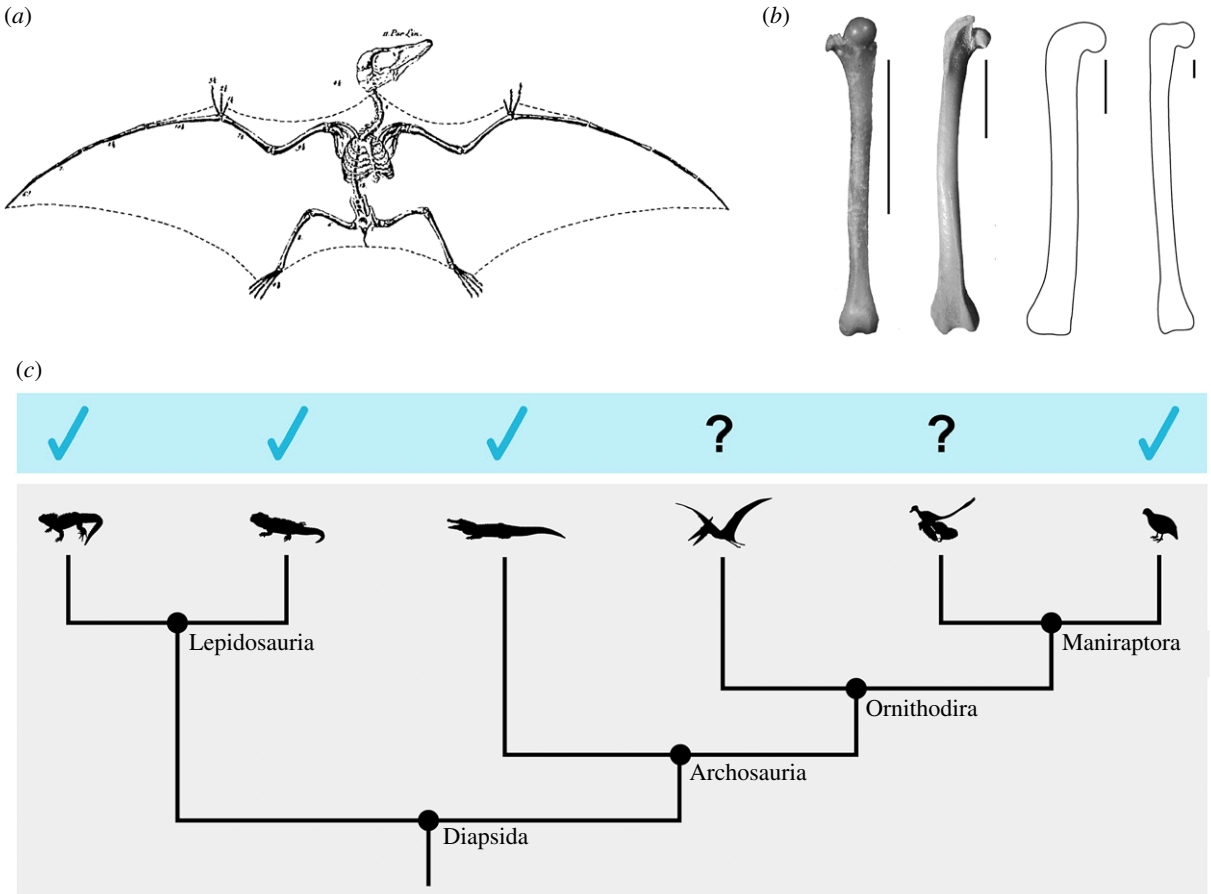

Figure 5. (*a*) Von Soemmering's [43] reconstruction of a juvenile *Pterodactylus* as a reptilian bat. (*b*) Right femora of *Eptesicus fuscus* (bat), *Coturnix coturnix* (quail), *Dimorphodon macronyx* (pterosaur; YPM 9182; after [44]) and *Microraptor hanqingi* (basal maniraptoran; IVPP V 12622; after [45]). Note the similarities in proximal femoral morphology among the ornithodirans, and the different orientation of the femoral head in the bat. Scale bar, 1 cm. (*c*) The phylogenetic framework used for inferences about hip capsular morphology in pterosaurs and basal maniraptorans. Blue ticks indicate knowledge of a ventral ligamentous thickening in the hip joint capsule based on existing dissections of extant diapsids. (Online version in colour.)

maniraptorans (including *Microraptor*) had the same ligamentous configuration as extant birds. No such analysis has yet been conducted for other extinct diapsids, but dissections by Tsai & Holliday [32] indicate that, despite differences in their pelvic morphology, *Sphenodon*, *Iguana*, *Alligator* and various birds all have ventral ligamentous thickenings of their hip joint capsules that originate from the ventral portion of the acetabulum (figure 5*c*). Thus, based on their phylogenetic position and proximal femoral morphology, it is most reasonable to infer that (whether or not this ligament is truly homologous to the avian ischiofemoral ligament) pterosaurs also had a ventral thickening in the joint capsule that originated from the ventral acetabulum and inserted, at least in part, on the medial femoral metaphysis. The fibres of this ligament would, as a result of their orientation, be primarily involved in limiting hip abduction.

It could be argued that even if an extinct ornithodiran also had a ligament placed in this way, its resting length or material properties could have been different from those of the common quail ischiofemoral ligament, such that it allowed larger excursions in ABAD than those measured in our study. There are no data available from the fossil record to test this statement. Our ability to determine the likelihood of such variation based on studies of ligaments in extant animals is limited, because their taxonomic sampling is generally biomedically driven, and they often focus on structural strain at failure (e.g. [57,58]; but see [59] for a discussion of physiological strain). If future studies find that the resting lengths or physiological strain values of hip capsular ligaments vary substantially among extant diapsids, particularly archosaurs, it would be plausible that they could have differed from the common quail in pterosaurs and basal maniraptorans, as well. However, considering the outcome of our dynamic ligament fibre simulation, these differences would have to be dramatic to facilitate a batlike level of hip joint abduction.

Even hypothetically allowing for variation in these parameters that would result in increased 'ligamentous' hip mobility in extinct ornithodirans (potentially at the cost of joint stability; see [55]), it must be borne in mind that ligaments are by no means the only structures that constrain joint mobility. Functional studies of extant taxa have demonstrated that muscles, tendons and integument further constrain joint mobility beyond what is possible with only joint capsules and ligaments intact (e.g. [12,33,35]). The poses used in a wide variety of *in vivo* behaviours form a still smaller subset of even that ROM (e.g. [19,24]). Therefore, future reconstructions of a batlike hip pose in pterosaurs or basal maniraptorans will not only require explanations for how the hip ligaments of these animals allowed increased abduction, but also for how their other soft tissues did not prevent this pose, as well as for how this pose was reached in life. Based on all available evidence and in the absence of extraordinary evidence to the contrary, we conclude that although the batlike hip pose proposed for extinct ornithodirans appears possible based on osteological manipulation, it was, in all probability, inviable.

(d) Potential applications of this methodology

We encourage interested workers to co-opt our methodology for their own purposes. To facilitate adjustment and use of our experimental methods, we have provided our Maya and MatLab scripts for systematically sampling joint poses, automatically checking for mesh model interpenetration, creating a ROM map, and dynamically simulating ligament fibres, as well as plain-English instructions for implementing them, as electronic supplementary material, methods S1–S4.

Although modifications will be necessary in order to apply our workflow for estimation of 'osteological' ROM to joints that are more prone to disarticulation than interpenetration (e.g. bicondylar joints), the instructions provided here offer a foundation. We suggest that studies using digital models to estimate joint mobility for extinct taxa (e.g. [10,60,61]) can now be automated to avoid inter-observer error, and their search parameters can be standardized and reported. Ligament fibre simulation in Maya (Autodesk, San Rafael, CA, USA) obviates the complex optimization algorithms (e.g. [62]) typically considered necessary to create ligament models that wrap around bones in a life-like manner, making this source of data accessible to a broader community of functional morphologists.

ROM maps can be used to address a variety of questions about joint mobility. These visualizations can be simply created for any joint, using 3D mobility data collected from digital manipulation of dry or cartilage-capped bone mesh models, or experiments involving cadaveric or living animals. By enabling a pose-based rather than an excursion-based analysis of joint motion, ROM mapping effectively captures the 3D complexity of joint mobility and allows more accurate comparisons of mobility data within and among taxa.

Ethics. All animal subjects used in this study were obtained as cadavers; no IACUC policy applies.

Data accessibility. The calibration images, X-ray videos and CT files used in this study are available on the X-ray Motion Analysis Research Portal (xmaportal.org, Study Identifier BROWN68).

Authors' contributions. A.R.M. and K.P. conceived of the study. A.R.M. designed the study and carried out the experiments and analyses. A.R.M. and K.P. drafted and edited the manuscript and gave final approval for publication.

Competing interests. We declare we have no competing interests.

Funding. This research was supported by funding from the Bushnell Research and Education Fund and Sigma Xi Grant-in-Aid of Research G2016100191859492 awarded to A.R.M., and funding from the Uplands Foundation and the Sakana Foundation to A.R.M. and K.P.

Acknowledgements. We thank Elizabeth Brainerd for access to laboratory equipment, Sharon Swartz for access to a specimen of *E. fuscus*, Jeremy Lomax for assistance with experiments, Henry Tsai for discussions about hip soft tissue anatomy, Stephen Gatesy for assistance with experiments and discussions about ROM that greatly improved the quality of this research, and John Hutchinson, Joel Hutson and two anonymous reviewers for their comments on the manuscript.

References

1. Bramwell CD, Whitfield GR. 1974 Biomechanics of *Pteranodon*. *Phil. Trans. R. Soc. Lond. B* **267**, 503–581. (doi:10.1098/rstb.1974.0007)
2. Robinson JA. 1975 The locomotion of plesiosaurs. *N. Jb. Geol. Palaeont. Abh.* **149**, 286–332.
3. Padian K. 1983 A functional analysis of flying and walking in pterosaurs. *Paleobiology* **9**, 218–239. (doi:10.1017/S009483730000765X)
4. Godfrey SJ. 1984 Plesiosaur subaqueous locomotion: a reappraisal. *N. Jb. Geol. Paläont. Abh* **11**, 661–672.
5. Senter P, Robins JH. 2005 Range of motion in the forelimb of the theropod dinosaur *Acrocanthosaurus atokensis*, and implications for predatory behaviour. *J. Zool.* **266**, 307–318. (doi:10.1017/S0952836905006989)
6. Horner JR, Padian K, de Ricqlès A. 2001 Comparative osteohistology of some embryonic and perinatal archosaurs: developmental and behavioral implications for dinosaurs. *Paleobiology* **27**, 39–58. (doi:10.1666/0094-8373(2001)027<0039:COOSEA>2.0.CO;2)
7. Bonnan MF, Sandrik JL, Nishiwaki T, Wilhite D, Elsey RM, Vittore C. 2010 Calcified cartilage shape in archosaur long bones reflects overlying joint shape in stress-bearing elements: implications for nonavian dinosaur locomotion. *Anat. Rec.* **293**, 2044–2055. (doi:10.1002/ar.21266)
8. Holliday CM, Ridgely RC, Sedlmayr JC, Witmer LM. 2010 Cartilaginous epiphyses in extant archosaurs and their implications for reconstruction limb function in dinosaurs. *PLoS ONE* **5**, e13120. (doi:10.1371/journal.pone.0013120)
9. Archer DB (ed.). 1999 *Biology of the synovial joint*. Abingdon, UK: Taylor & Francis.
10. Pierce SE, Clack JA, Hutchinson JR. 2012 Three-dimensional limb joint mobility in the early tetrapod *Ichthyostega*. *Nature* **486**, 523–526. (doi:10.1038/nature11124)
11. Carpenter K, Wilson Y. 2008 A new species of *Camptosaurus* (Ornithopoda: Dinosauria) from the Morrison Formation (Upper Jurassic) of Dinosaur National Monument, Utah, and a biomechanical analysis of its forelimb. *Ann. Carnegie Mus.* **76**, 227–263. (doi:10.2992/0097-4463(2008)76[227:ANSOCO]2.0.CO;2)
12. Hutson JD, Hutson KN. 2012 A test of the validity of range of motion studies of fossil archosaur elbow mobility using repeated-measures analysis and the extant phylogenetic bracket. *J. Exp. Biol.* **215**, 2030–2038. (doi:10.1242/jeb.069567)
13. Hutson JD, Hutson KN. 2013 Using the American alligator and a repeated measures design to place constraints on *in vivo* shoulder joint range of motion in dinosaurs and other fossil archosaurs. *J. Exp. Biol.* **216**, 275–284. (doi:10.1242/jeb.074229)
14. Hutson JD, Hutson KN. 2014 A repeated-measures analysis of the effects of soft tissues on wrist range of motion in the extant phylogenetic bracket of dinosaurs: implications for the functional origins of an automatic wrist folding mechanism in *Crocodilia*. *Anat. Rec.* **297**, 1228–1249. (doi:10.1002/ar.22903)
15. Hutson JD, Hutson KN. 2015 Inferring the prevalence and function of finger hyperextension in Archosauria from finger-joint range of motion in the American alligator. *J. Zool.* **296**, 189–199. (doi:10.1111/jzo.12232)
16. Hutson JD, Hutson KN. 2015 An examination of forearm bone mobility in *Alligator mississippiensis* (Daudin, 1802) and *Struthio camelus* Linnaeus, 1758 reveals that *Archaeopteryx* and dromaeosaurs shared an adaptation for gliding and/or flapping. *Geodiversitas* **37**, 325–344. (doi:10.5252/g2015n3a3)
17. Hutson JD, Hutson KN. 2018 Retention of the flight-adapted avian finger-joint complex in the ostrich helps identify when wings began evolving in dinosaurs. *Ostrich*, 1–14. (doi:10.2989/00306525.2017.1422566)
18. Cobley MJ, Rayfield EJ, Barrett PM. 2013 Inter-vertebral flexibility of the ostrich neck: implications for estimating sauropod neck flexibility. *PLoS ONE* **8**, e72187. (doi:10.1371/journal.pone.0072187)
19. Arnold P, Fischer MS, Nyakatura JA. 2014 Soft tissue influence on *ex vivo* mobility in the hip of *Iguana*: comparison with in vivo movement and its bearing on joint motion of fossil sprawling tetrapods. *J. Anat.* **225**, 31–41. (doi:10.1111/joa.12187)
20. Manafzadeh AR, Padian K. 2016 Could pterosaurs adopt a batlike wing pose? Implications of a functional analysis of the avian hip ligaments for the evolution of ornithodiran stance and gait. In *SVP 2016: Meeting program and abstracts*, p. 183. See http://vertpaleo.org/2016-Annual-Meeting/Annual-Meeting-Home.aspx.
21. Witmer LM. 1995 The extant phylogenetic bracket and the importance of reconstructing soft tissues in fossils. In *Functional morphology in vertebrate*

paleontology (ed. JJ Thomason), pp. 19–33. New York: NY: Cambridge University Press.

22. Haines RW. 1942 The evolution of epiphyses and of endochondral bone. *Biol. Revs.* **17**, 267–292. (doi:10.1111/j.1469-185X.1942.tb00440.x)
23. Haines RW. 1942 The tetrapod knee joint. *J. Anat.* **76**, 270–301.
24. Kambic RE, Roberts TJ, Gatesy SM. 2017 3-D range of motion envelopes reveal interacting degrees of freedom in avian hind limb joints. *J. Anat.* **231**, 906–920. (doi:10.1111/joa.12680)
25. Livezey BC, Zusi RL. 2007 Higher-order phylogeny of modern birds (Theropoda, Aves: Neornithes) based on comparative anatomy. II. Analysis and discussion. *Zool. J. Linnaean Soc.* **149**, 1–95. (doi:10.1111/j.1096-3642.2006.00293.x)
26. Brainerd EL, Baier DB, Gatesy SM, Hedrick TL, Metzger KA, Gilbert SL, Crisco JJ. 2010 X-ray reconstruction of moving morphology (XROMM): precision, accuracy and applications in comparative biomechanics research. *J. Exp. Zool. A* **313**, 262–279. (doi:10.1002/jez.589)
27. Knörlein BJ, Baier DB, Gatesy SM, Laurence-Chasen JD, Brainerd EL. 2016 Validation of XMALab software for marker-based XROMM. *J. Exp. Biol.* **219**, 3701–3711. (doi:10.1242/jeb.145383)
28. Kambic RE, Roberts TJ, Gatesy SM. 2014 Long-axis rotation: a missing degree of freedom in avian bipedal locomotion. *J. Exp. Biol.* **217**, 2770–2782. (doi:10.1242/jeb.101428)
29. Grood ES, Suntay WJ. 1983 A joint coordinate system for the clinical description of three-dimensional motions: application to the knee. *J. Biomech. Eng.* **105**, 136–144. (doi:10.1115/1.3138397)
30. Halilaj E, Rainbow MJ, Moore DC, Laidlaw DH, Weiss APC, Ladd AL, Crisco JJ. 2015 In vivo recruitment patterns in the anterior oblique and dorsoradial ligaments of the first carpometacarpal joint. *J. Biomech.* **48**, 1893–1898. (doi:10.1016/j.jbiomech.2015.04.028)
31. Baumel JJ, Raikow RJ. 1993 Arthrologia. In *Handbook of avian anatomy: nomina anatomica avium* (eds JJ Baumel, AS King, JE Breazile, HE Evans, JC Vanden Berge), 2nd edn, pp. 133–187. Cambridge, MA: Nuttall Ornithological Club.
32. Tsai HP, Holliday CM. 2015 Articular soft tissue anatomy of the archosaur hip joint: structural homology and functional implications. *J. Morph.* **276**, 601–630. (doi:10.1002/jmor.20360)
33. Stolpe M. 1932 Physiologisch-anatomische Untersuchungen über die hintere Extremität der Vögel. *J. für Ornithologie.* **80**, 161–247. (doi:10.1007/BF01908701)
34. Cracraft J. 1971 Functional morphology of the hind limb of the domestic pigeon, *Columba livia*. *Amer. Mus. Nat. Hist. Bull.* **144**, 173–268.
35. Firbas W, Zweymüller K. 1971 Über das Hüftgelenk der Ratiten. *Gegenbaurs Morph. Jahrb* **116**, 91–103.
36. Rankin JW, Rubenson J, Hutchinson JR. 2016 Inferring muscle functional roles of the ostrich pelvic limb during walking and running using computer optimization. *J. R. Soc. Interface* **13**, 20160035. (doi:10.1098/rsif.2016.0035)
37. Bryant HN, Russell AP. 1992 The role of phylogenetic analysis in the inference of unpreserved attributes of extinct taxa. *Phil. Trans. R. Soc. Lond. B* **337**, 405–418. (doi:10.1098/rstb.1992.0117)
38. Tsai HP, Middleton KM, Hutchinson JR, Holliday CM. 2018 Hip joint articular soft tissues of non-dinosaurian *Dinosauromorpha* and early *Dinosauria*: evolutionary and biomechanical implications for Saurischia. *J. Vertebr. Paleontol.* **38**, e1427593. (doi:10.1080/02724634.2017.1427593)
39. Wellnhofer P. 1975 Die Rhamphorhynchoidea (Pterosauria) der Oberjura-Plattenkalke Süddeutschlands, Teil III: Palökologie und Stammesgeschichte. *Palaeontogr. Abt. A*, 1–30.
40. Unwin DM. 1996 Pterosaur tracks and the terrestrial ability of pterosaurs. *Lethaia* **29**, 373–386. (doi:10.1111/j.1502-3931.1996.tb01673.x)
41. Wilkinson MT, Unwin DM, Ellingtton CP. 2006 High lift function of the pteroid bone and forewing of pterosaurs. *Proc. R. Soc. B* **273**, 119–126. (doi:10.1098/rspb.2005.3278)
42. Elgin RA, Hone DWE, Frey E. 2011 The extent of the pterosaur flight membrane. *Acta Palaeontol. Pol.* **56**, 99–111. (doi:10.4202/app.2009.0145)
43. Von Soemmering T. 1817 Über einen Ornithocephalus brevirostris der Vorwelt, Denkschriften der königlichen bayerischen Akademie der Wissenschaften, Math.-Phys. *Klasse* **6**, 89–104.
44. Padian K. 1983 Description and reconstruction of new material of *Dimorphodon macronyx* (Buckland) (Pterosauria: Rhamphorhynchoidea) in the Yale Peabody Museum. *Postilla* **189**, 1–44.
45. Gong EP, Martin LD, Burnham DA, Falk AR, Hou LH. 2012 A new species of *Microraptor* from the Jehol Biota of northeastern China. *Palaeoworld* **21**, 81–91. (doi:10.1016/j.palwor.2012.05.003)
46. Taquet P, Padian K. 2004 The earliest known restoration of a pterosaur and the philosophical origins of Cuvier's Ossemens Fossiles. *C.R. Palevol* **3**, 157–175. (doi:10.1016/j.crpv.2004.02.002)
47. Beebe W. 1915 A tetrapteryx stage in the ancestry of birds. *Zoologica* **2**, 39–52.
48. Alexander DE, Gong E, Martin LD, Burnham DA, Falk AR. 2010 Model tests of gliding with different hindwing configurations in the four-winged dromaeosaurid *Microraptor gui*. *Proc. Natl Acad. Sci. USA* **107**, 2972–2976. (doi:10.1073/pnas.0911852107)
49. Stuelpnagel J. 1964 On the parameterization of the three-dimensional rotation group. *SIAM Rev.* **6**, 422–430. (doi:10.1137/1006093)
50. Padian K. 1991 Pterosaurs: were they functional birds or functional bats? In *Biomechanics and evolution* (eds JMV Rayner, RJ Wootton), pp. 146–160. Cambridge, UK: Cambridge University Press.
51. Cheney JA, Ton D, Konow N, Riskin DK, Breuer KS, Swartz SM. 2014 Hindlimb motion during steady flight of the lesser dog-faced fruit bat, *Cynopterus brachyotis*. *PloS ONE* **9**, e98093. (doi:10.1371/journal.pone.0098093)
52. Carrano MT. 2000 Homoplasy and the evolution of dinosaur locomotion. *Paleobiology* **26**, 489–512. (doi:10.1666/0094-8373(2000)026<0489:HATEOD>2.0.CO;2)
53. Hutchinson JR. 2001 The evolution of femoral osteology and soft tissues on the line to extant birds (Neornithes). *Zool. J. Linn. Soc.* **131**, 169–197. (doi:10.1111/j.1096-3642.2001.tb01314.x)
54. Wellnhofer P. 1978 *Handbuch der Paläoherpetologie. Teil 19: Pterosauria*. Stuttgart, Germany: Gustav Fischer Verlag.
55. Nordin M, Frankel VH (eds). 2001 *Basic biomechanics of the musculoskeletal system*. Philadelphia, PA: Lippincott Williams & Wilkins.
56. Tsai HP. 2015 Archosaur hip joint anatomy and its significance in body size and locomotor evolution. Dissertation, University of Missouri–Columbia, Columbia, MO.
57. Bigliani LU, Kelkar R, Flatow EL, Pollock RG, Mow VC. 1996 Glenohumeral stability: biomechanical properties of passive and active stabilizers. *Clin. Orthop. Rela. Res.* **330**, 13–30. (doi:10.1097/00003086-199609000-00003)
58. Hewitt J, Guilak F, Glisson R, Vail TP. 2001 Regional material properties of the human hip joint capsule ligaments. *J. Orthop. Res.* **19**, 359–364. (doi:10.1016/S0736-0266(00)00035-8)
59. Beynnon BD, Fleming BC. 1998 Anterior cruciate ligament strain in-vivo: a review of previous work. *J. Biomech.* **31**, 519–525. (doi:10.1016/S0021-9290(98)00044-X)
60. Otero A, Allen V, Pol D, Hutchinson JR. 2017 Forelimb muscle and joint actions in Archosauria: insights from *Crocodylus johnstoni* (Pseudosuchia) and *Mussaurus patagonicus* (Sauropodomorpha). *PeerJ* **5**, e3976. (doi:10.7717/peerj.3976)
61. Lai PH, Biewener AA, Pierce SE. 2018 Three-dimensional mobility and muscle attachments in the pectoral limb of the Triassic cynodont *Massetognathus pascuali* (Romer, 1967). *J. Anat.* **62**, 383–406. (doi:10.1111/joa.12766)
62. Marai GE, Laidlaw DH, Demiralp C, Andrews S, Grimm CM, Crisco JJ. 2004 Estimating joint contact areas and ligament lengths from bone kinematics and surfaces. *IEEE Trans. Biomed. Eng.* **51**, 790–799. (doi:10.1109/TBME.2004.826606)